Proceedings of the International Gas Turbine Congress 2003 Tokyo
November 2-7, 2003

IGTC2003Tokyo TS-078

Rib-Induced Secondary Flow Structures inside a High Aspect Ratio Trapezoidal Channel

- Application to Cooling of Gas Turbine Blade Trailing Edge –

Robert KIML, Sadanari MOCHIZUKI, Akira MURATA and Matej SULITKA

Tokyo University of A&T, Department of Mechanical Systems Engineering
Nakacho 2-24-16, Koganei-shi, Tokyo, JAPAN
Phone/Fax: +81-42-388-7088, E-mail: robert@mmlab.mech.tuat.ac.jp

ABSTRACT

Heat flow visualization experiment and numerical simulation were performed in a trapezoidal high aspect ratio channel representing a turbine blade trailing edge cooling passage. The transverse and oblique ribs were attached to two opposing long side walls and they were intended to function as secondary flow inducers as well as turbulators in order to improve the heat transfer of the both rib-roughened and Rear (shorter one of the short side walls) walls. The experiments and simulations were performed for four different rib inclinations, 90, 75, 60 and 45-deg. ribs respectively, and two types of ribs, proportional and non-proportional ribs, respectively. The rib proportionality was based on the trapezoidal shape of the channel, so that the ratio of the rib height to the local channel width in the vertical direction was always equal to 1/3. The "non-proportional ribs" had a square cross section with rib height e=1/3w. The obtained results present a complicated flow structure with a rib-induced secondary flow which conveyed the air form the passage core region towards the Rear wall. They also confirmed that rib shape and rib inclination play a dominant role in determining the optimal flow distribution inside the trapezoidal trailing edge cooling channel.

INTRODUCTION

Effective use of today's energy resources and in particular the need for the environment friendly energy requires a more efficient use of the existing energy resources. One of the examples of an invention and rapid development in this field is a gas turbine engine; a device widely used in marine, airline and power generation industries for its high performance and high efficiency. It is well known that the efficiency of such an engine can be greatly enhanced if the turbine inlet gas temperature is increased. However, the presently available materials with high heat resistance can not protect the vital turbine components sufficiently yet. Therefore, they must be provided with cooling techniques such as forced convection cooling, impingement cooling, film cooling and their combinations.

Among numerous heat transfer enhancement techniques ribs are most widely employed to augment the heat transfer performance inside cooling channels. The mechanism of the heat transfer enhancement by the conventional ribs is based on the flow separation and reattachment as can be well demonstrated by the transverse ribs (ribs perpendicular to the main flow direction) that induce two-dimensional flow phenomenon. When heat is transferred from the wall to the flowing fluid inside the flow channel, fluid temperature in the core region is always lower than that near the wall. Accordingly, if the cold and higher momentum fluid in the central core region of the channel is by some means carried to the hot area near the wall, heat transfer will be enhanced. In other words, if the secondary flow occurs, the thickness of both velocity and thermal boundary layers on the wall where the flow from the channel core region hits will become thinner and the heat transfer in that region will be augmented.

Manuscript Received on April 4, 2003

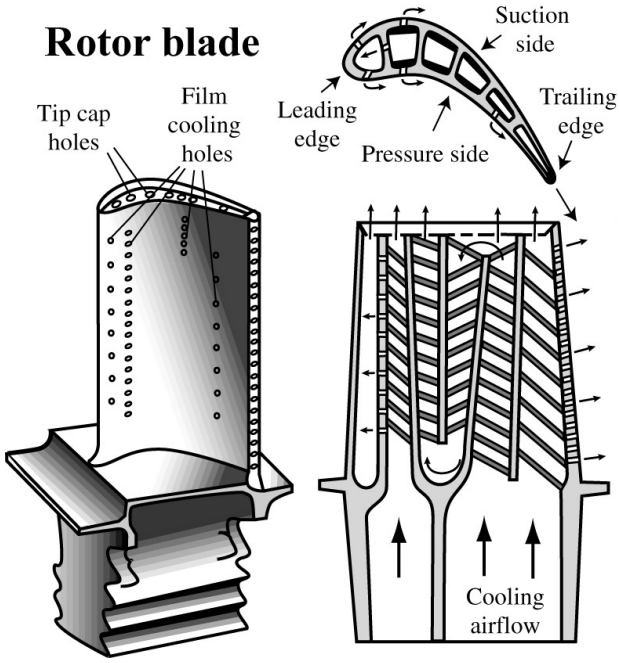

Fig. 1 Schematic of external and internal gas turbine rotor blade structure.

The internal cooling of gas turbine blades has been already studied by many scientists. For example, studies by Han, (1984), Han et al., (1985), Kiml et al., (2000), Mochizuki et al., (1997), Murata et al., (1994), Rau et al., (1996) and Kiml et al., (2001) studied the heat transfer and pressure drop characteristics in rib-roughened passages with different rib arrangements. They focused on the effects of the Reynolds number and the rib geometry on heat transfer and pressure drop in the fully developed region of uniformly heated square and rectangular channels. All these studies also showed that the secondary flow induced by the rib inclination augmented heat transfer better than the two dimensional flow

phenomena induced by the transverse ribs. Further studies by Dutta et al., (1996), El-Husayni et al., (1994), Johnson et al., (1993), Murata and Mochizuki, (2001), Taslim et al., (1991), Wagner et al., (1992) and Kiml et al., (2001) examined the effects of Coriolis force, centrifugal force and buoyancy force on the heat transfer characteristics with different rib configurations. The effects of the 180-degree sharp turn on the flow, pressure drop and heat transfer in a serpentine passage have been reported by Cheng et al., (1992), Cardone et al., (1998), Kiml et al., (1998) and Metzger et al., (1984). Studies by Dutta, S et al., (1995), Ekkad and Han, (1997), Han et al., (1991), Han and Zhang, (1992), Hu and Shen, (1996), Johnson et al., (1994), Kawaike et al., (1995), Taslim et al., (1994) and Kiml et al., (2001) presented the heat transfer results for the parallel, staggered, broken, crossed and V-shaped rib patterns. However, with the advancement of gas turbine technology it became necessary to focus the attention on the regions exposed to the most severe thermal conditions, leading and trailing edges, as shown in Fig. 1. In particular, the trailing edge, due to its significant shortage of cooling space for the internal cooling, is becoming one of the most important problems to realize more effective gas turbine engines. In order to cool the trailing edge of a blade, the installation of oblique ribs in the internal passage near the trailing edge as secondary-flow inducers as well as turbulators could be one solution. Recently, studies by Hirota et al., (1996), Kiml et al., (2000), Kiml et al., (2001), Taslim, et al., (1995), Taslim et al., (1997) and Zhang et al., (1994) showed the heat transfer data for the ribbed rectangular channels, which were partially similar (in aspect ratio) to the ones used in the present study. However, the authors investigated channels with different geometrical proportions and rib shape and they did not pay attention to the local flow structure induced by the ribs.

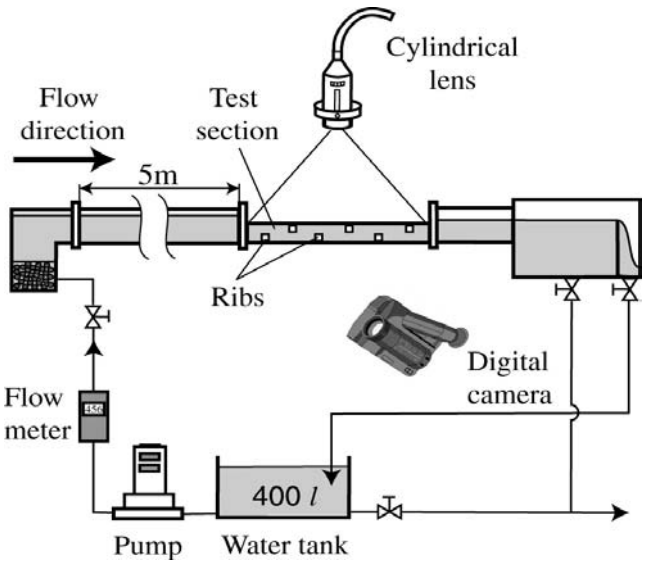

Fig. 2 Schematic of flow visualization experimental apparatus.

The present study focuses on detailed examination of the flow behavior inside a high aspect ratio rib-roughened trapezoidal cooling channel (corresponding to a real cooling passage inside a turbine blade). The emphasis is placed on the experimental and numerical investigation of the rib-induced flow structures with two different types of ribs and four different rib inclinations.

EXPERIMENTAL APPARATUS AND METHODS

Flow Visualization Experiment

The flow visualization using fine particles as tracers was carried out in a 6 m long water channel with a test section located 5 m downstream of the settling chamber (see Fig. 2). The test section with a trapezoidal cross section (detail view is presented in Fig. 3, w=30mm) was made of 10 mm thick transparent Plexiglas plates.

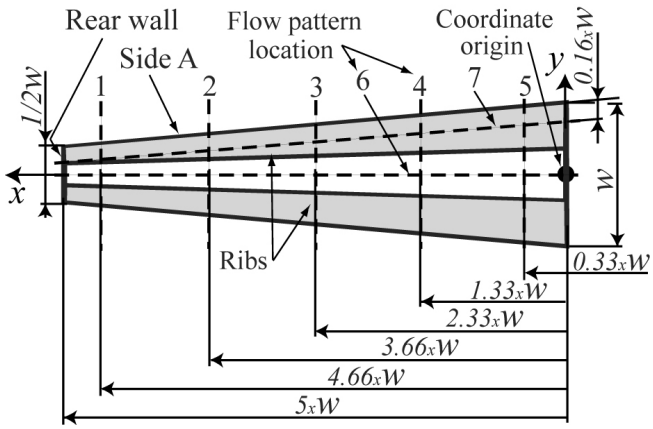

Fig. 3 Location of side and top view flow patterns inside a trapezoidal test section with proportional ribs.

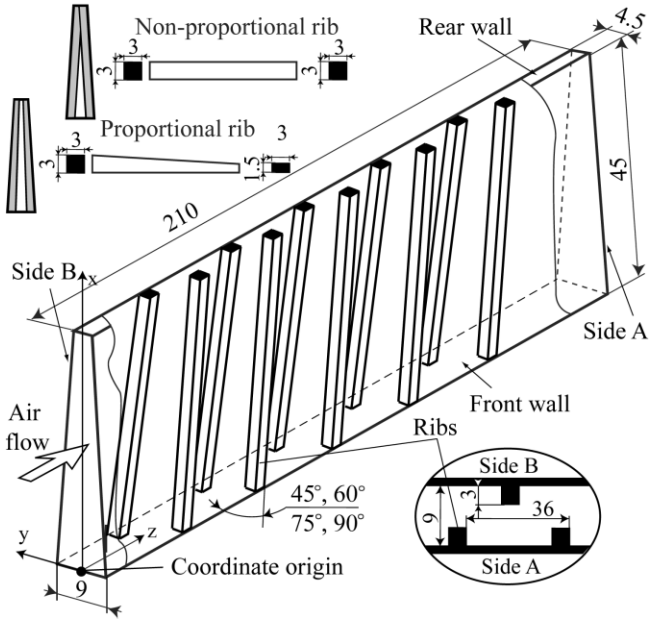

Fig. 4 Schematic of test section examined by the numerical simulation.

Water was mixed with the chemical compound $NaSO_4$, in order to increase the specific weight of the water to that of the particles. The particles (0.2 mm in diameter) were illuminated between the 5th and 7th ribs by an argon laser light-sheet (3 mm wide) and photographed by a still digital camera. The camera exposure time was set to 0.5 second to allow the creation of path lines by particles. In order to simplify the understanding of complicated flow structures induced by the ribs, the ribbed walls of the test section were named as Side A" and "Side B" whereas the smooth walls as "Rear" and "Front", as illustrated in Figs. 3 and 4.

Side view patterns were photographed at 5 locations x = 0.33w (near-Front wall region), 1.33w, 2.33w (center), 3.66w and 4.66w (near-Rear wall region) from the Front wall surface. Top view patterns were obtained at y = 0.16w (near-Side A region) and y=0w (central vertical plane) from the Side A wall surface. The ribs were made of transparent Plexiglas and mounted on two opposite walls of the channel. Four rib inclinations, 90, 75, 60 and 45-deg. ribs respectively, and two types of ribs, proportional and non-proportional ribs, respectively, were examined. The proportionality of so called "proportional ribs" was based on the trapezoidal shape of the channel, so that the ratio of the rib height to the local channel width in the vertical direction was always equal 1/3, as schematically depicted in Figs. 3 and 4. The

"non-proportional ribs" had a square cross section along the entire rib with rib height e=1/3w.

The flow visualization was performed in an enlarged test section with w=30mm while the numerical simulation in a test section with w=9 mm. The numerical simulation used the same dimensions with those used in the heat transfer experiments, results of which are not available yet.

Numerical Simulation

A numerical study of the flow field in a rib-roughened trapezoidal channel with ribs mounted on two longer side walls (see Fig. 4) has been performed using the finite volume FLUENT code (commercially available software, version 5.4). The procedure of solving the governing equations of continuity, momentum and energy is pressure-based, whereby the full Navier-Stokes equations are treated in general, body fitted coordinates. Control-volume storage scheme is employed where all variables are stored at the cell center. Second-order upwind scheme was used in this study in order to interpolate the face values of computed variables. A point implicit (Gauss-Seidl) linear equation solver is used in conjunction with algebraic multigrid (AMG) method to solve the resultant system of equations for the dependent variable in each cell. Implicit segregated solver solves the governing equations sequentially. In this study pressure-velocity coupling algorithm SIMPLE (Semi-Imlicit Method for Pressure-Linked Equations) was used.

The calculations were performed using the RSM (Reynolds Stress Model) model of turbulence. The individual Reynolds stresses are calculated from differential transport equations. These transport equations contain triple order velocity correlations and pressure-velocity correlations that have to be modeled (Turbulent Diffusion, Buoyancy Production, Pressure Strain and Dissipation). The near-wall values of Reynolds stresses and Dissipation rate on the surface were computed from wall functions. Explicit wall boundary conditions for Reynolds stresses were applied by using the log-law and the assumption of equilibrium. Turbulent kinetic energy is obtained via the transport equation. For the near wall treatment, standard wall functions were used to compute the shear stresses.

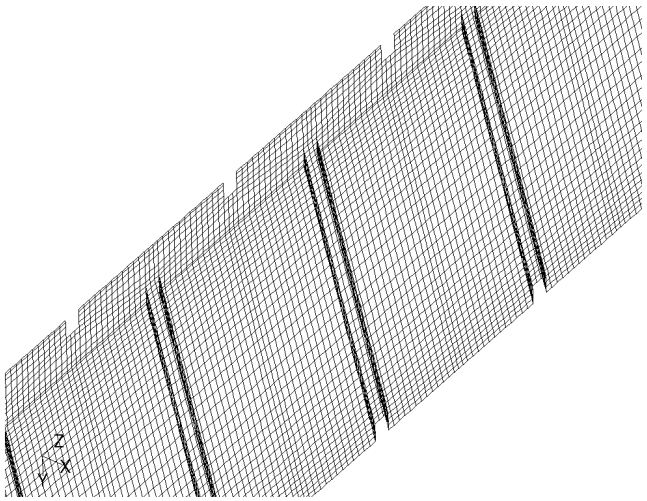

Fig. 5 A structural mesh for high aspect ratio trapezoidal test section with 90-deg. proportional ribs.

A structured mesh for the calculations was created with the size of first layer of computational cells so that the wall function would be $y+$ = max. 60. Grid density in the cross-section of the channel was 35x10 cells, as can be seen in the Fig. 5. At the inlet, a uniform velocity profile was set. Calculations have been performed for the inlet velocity of v_{in} = 20.4 m/s, with the corresponding Reynolds number (relative to the hydraulic diameter of the channel d_e = 11.7 mm) of Re = 15000. Reynolds stresses at the inlet were derived from the assumption of isotropy turbulence. Intensity of turbulence at the inlet was set to be Tu = 3%. At the outlet a fully developed velocity profile with zero gradients in the flow direction was assumed. All geometric proportions of the channel and ribs correspond with those used in the flow visualization experiments.

RESULTS AND DISCUSSION

As known from the previous studies, the 90-deg ribs induce fundamentally two-dimensional flow phenomenon with flow separation and reattachment taking place between two consecutive ribs. However, this knowledge applies only to the square or rectangular cross sectional flow channels. In the case of the trapezoidal flow channel the shape effects on the flow structure have to be taken in consideration.

For this reason the simulations were first conducted inside a smooth channel. The results showed that, in comparison to the rectangular channel with the same aspect ratio, the flow distribution within the trapezoidal channel cross section is not even and the larger volume of air transfer occurs in the wider part of the channel (in the near Front wall vicinity). This was caused by the boundary layer growth in the narrower part, which limited the mass transfer at this region. If the ribs are mounted on the two opposite sides of the trapezoidal channel, the boundary layer will be diminished and the main flow stream forced to meander among the ribs and redistribute the air flow more evenly than in the case of the smooth passage. As a result of this knowledge, two types of ribs were examined; proportional and non-proportional ribs, representing the most fundamental differences occurring inside the trapezoidal cross sectional flow channel.

90-deg. Proportional and Non-Proportional Ribs

The numerical simulation results for 90-deg. proportional and non-proportional ribs are presented in Figs. 6 and 7. The flow visualization results for these two cases demonstrated the same flow structures with those presented in these figures. Therefore, due to the space limitation given to this paper they are not presented here.

In both cases, 90-deg. proportional and non-proportional ribs, respectively, the main flow stream reattached between the ribs while creating a considerably large flow separations just behind the ribs. The proportion of these flow separations in comparison to the area taken by the main flow stream is almost constant in case of non-proportional ribs (see Fig. 6). (The locations of the side view flow patterns are presented in Figs. 3 and 6d) The local rib height to channel width ratio for the non-proportional ribs increases from 1/3 at the Front wall to 2/3 at the Rear wall. This creates a significant space reduction for the air flow near the Rear wall which results in an air movement towards the Front wall and creation of secondary flow in form of a vertical counterclockwise vortex just behind the ribs at the near Rear wall regions (see Fig. 6d1). The rib height and the location of the rib mounted on the opposite Side B wall also play a dominant role in determining the size of the flow separation and flow velocity near the Side A wall. This can be observed by the decreasing velocity vectors size in the spanwise direction, the largest being near the Rear wall and the shortest near the Front wall, respectively, and opposite flow directions (a flow separation border line) occurring just in front of the rib mounted on the opposite Side B wall. A similar vortex can be also observed in the case of proportional ribs (see Fig. 7d). However here it is much weaker and it occupies a larger area. The flow is more evenly redistributed throughout the entire flow channel with a higher flow velocity and a larger air volume transferred to the near Rear wall region in comparison the non-proportional ribs. In addition, the proportion of the flow separations in comparison to the area taken by the main flow stream considerably decreases with distance from the Front wall for the proportional ribs, as can be confirmed by comparing Figs. 7a and 7c. The ribs' proportional shape induces a considerably better air distribution and mass transfer near the Rear wall unseen in a smooth trapezoidal channel (see Figs. 7d and 7e).

Non-Proportional ribs

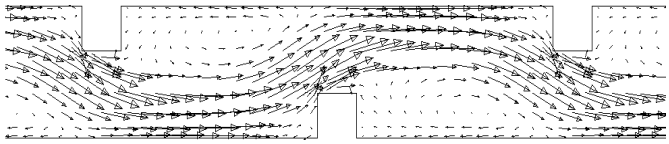

a) Flow pattern taken at $x = 0.33w$ (near-Front wall region).

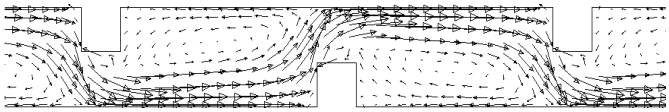

b) Flow patter taken at $x=2.33w$ (central vertical plane).

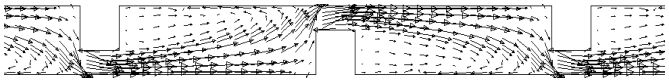

c) Flow patter taken at $x=4.66w$ (near-Rear wall region).

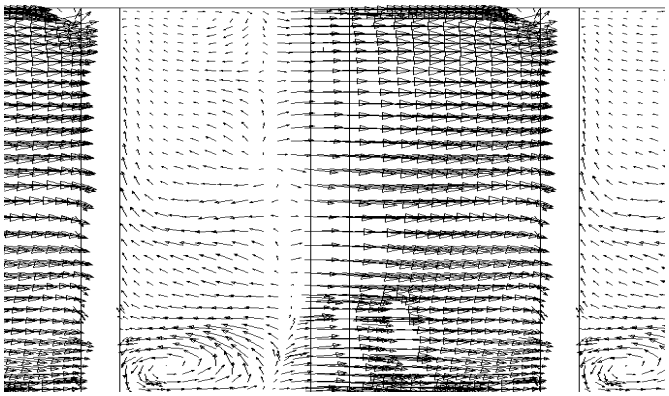

d) Flow pattern taken at $y = 0.16w$ (near-Side A region).

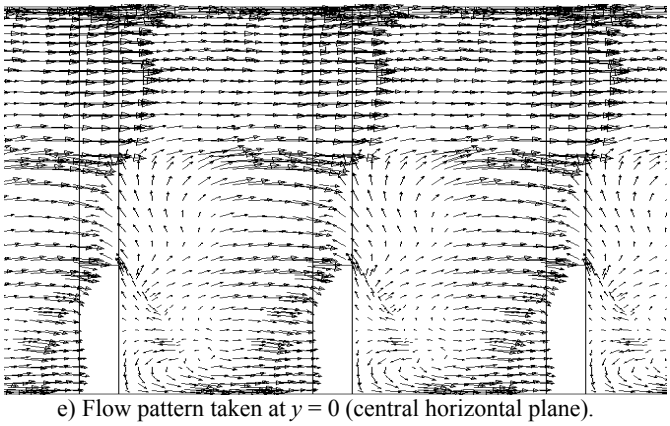

e) Flow pattern taken at $y = 0$ (central horizontal plane).

Fig. 6 Velocity vector distribution between 6th and 7th consecutive ribs for 90-deg. non-proportional ribs, *Re*=15,000.

Proportional ribs

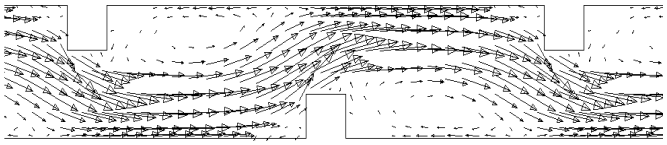

a) Flow pattern taken at $x = 0.33w$ (near-Front wall region).

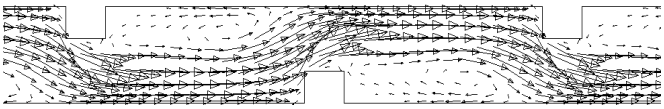

b) Flow patter taken at $x=2.33w$ (central vertical plane).

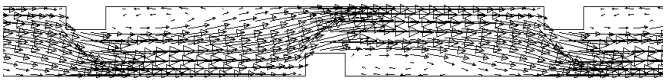

c) Flow patter taken at $x=4.66w$ (near-Rear wall region).

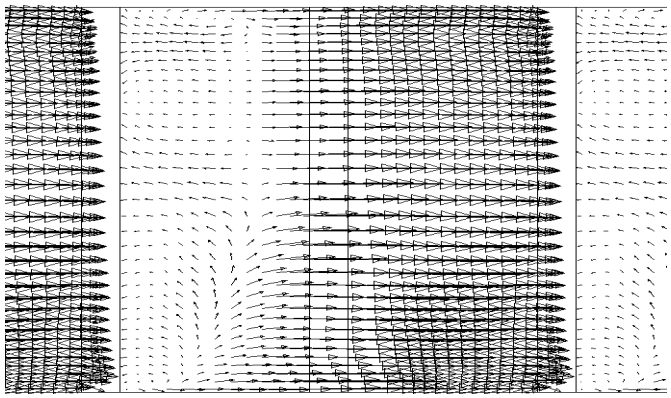

d) Flow pattern taken at $y = 0.16w$ (near-Side A region).

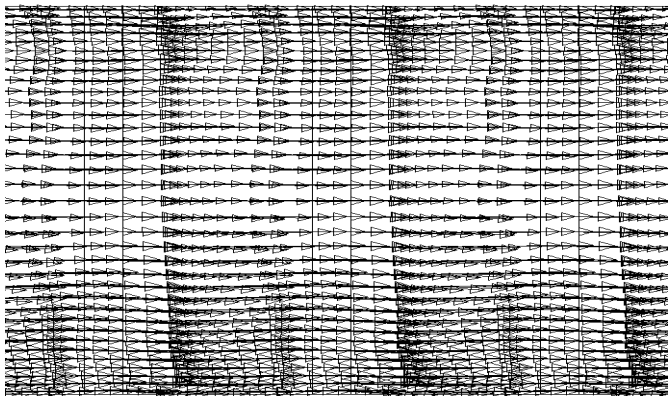

e) Flow pattern taken at $y = 0$ (central horizontal plane).

Fig. 7 Velocity vector distribution between 6th and 7th consecutive ribs for 90-deg. proportional ribs, *Re*=15,000.

60-deg. Non-Proportional Ribs

The results from flow visualization experiment and numerical simulation for the 60-deg. non-proportional ribs are presented in Fig. 8. In case of the flow visualization results (Figs. 8d1 and 8e1) the reader can see not only the ribs mounted on the Side A, a wall closer to the reader (ribs numbered as 5th, 6th and 7th rib), but also the ribs mounted on the opposite Side B wall. That was caused by the close distance between the ribs and limited transfer of light through the ribs. The results from the numerical simulation also show the counters of the ribs on opposite Side B (see Fig. 8d2), however, in this case one can clearly distinguish areas with air flow (velocity vectors) and white areas representing the rib.

It can be clearly observed in these figures that the main flow stream meanders among the ribs, reattaches between them and creates large separation regions just behind the ribs as was observed for the 90-deg. non-proportional ribs. However, in a closer look at the local flow structure one can see that from the reattachment point the flow proceeds in a direction towards the Rear wall with a gradual inclination increase of the flow velocity vectors with a decreasing distance to the Rear wall, as shown in Figs. 8d1 and 8d2. Opposite flow direction, towards the Front wall, respectively, is clearly visible inside the flow separation. In contrast to the 90-deg. ribs where the secondary flow was induced by the trapezoidal shape of the flow channel, the 60-deg. inclined ribs induce a secondary flow, which conveys the air from the channel core region towards the Rear wall. The secondary flow pushes larger volume of air towards the Rear wall and partially reduces the strength and velocity of the flow near the Front wall (compare Figs. 8a2 and 6a).

60-deg. Non-Proportional Ribs

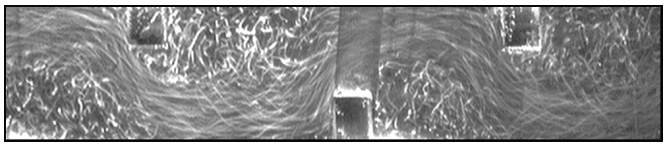

a1) Flow pattern taken at $x = 0.33w$ (near-Rear wall region).

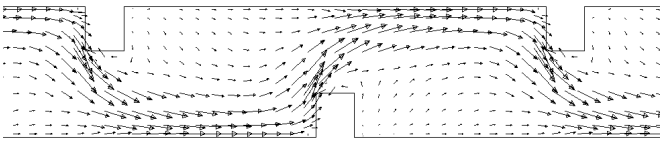

a2) Flow pattern taken at $x = 0.33w$ (near-Rear wall region).

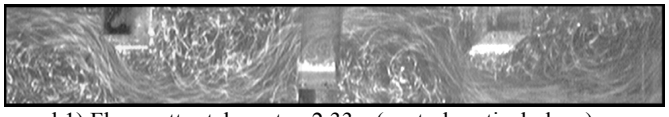

b1) Flow patter taken at x=2.33w (central vertical plane).

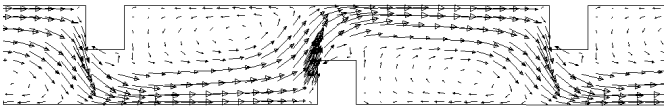

b2) Flow patter taken at x=2.33w (central vertical plane).

c1) Flow patter taken at x=4.66w (near-Front wall region).

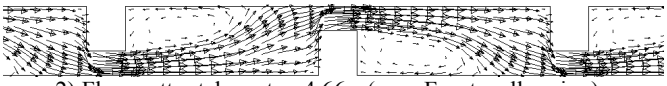

c2) Flow patter taken at x=4.66w (near-Front wall region).

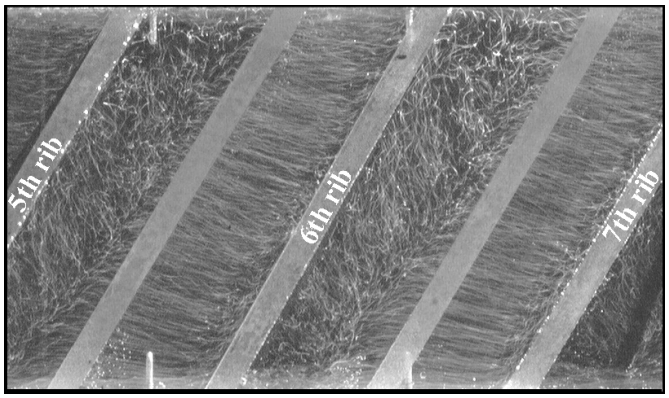

d1) Flow pattern taken at $y = 0.16w$ (near-Side A region).

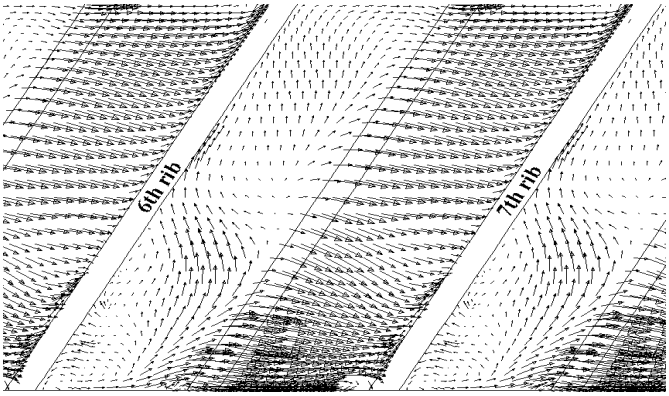

d2) Flow pattern taken at $y = 0.16w$ (near-Side A region).

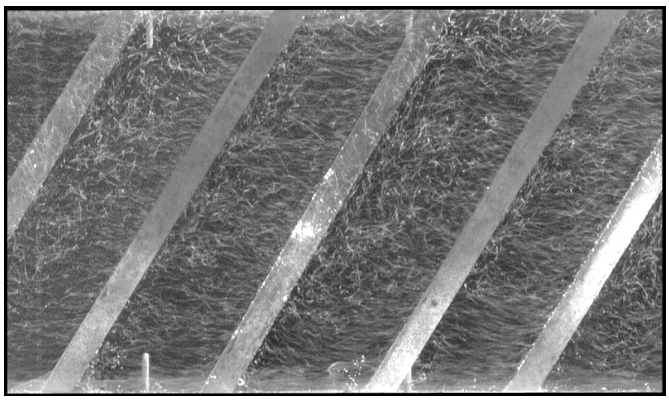

e1) Flow pattern taken at $y = 0$ (central horizontal plane).

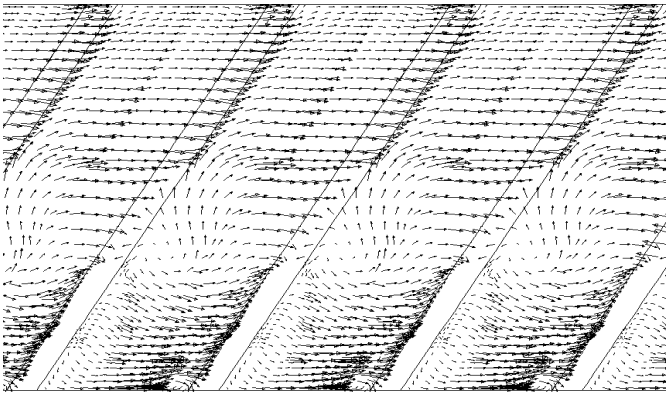

e2) Flow pattern taken at $y = 0$ (central horizontal plane).

Fig. 8 Velocity vector distribution between consecutive ribs for 60-deg. non-proportional ribs, *Re*=15,000.

Cross sectional views of this complicated secondary flow field between the 5th and 7th ribs are shown in Fig. 9. It can be clearly observed in this figure that the flow inside the trapezoidal channel can be divided into two major flow fields, a clockwise vortex taking place between the 5th rib on the Side B and 5th rib on the Side A and a counterclockwise vortex between the 5th rib on the Side A and 6th rib on the Side B, respectively (Side A is an upper wall from the reader's perspective). The same flow structure repeats between all consecutive ribs. Both vortices characterize the flow separation near one wall and flow reattachment on the opposite wall. Half of each vortex consists of the flow separation with the flow proceeding towards the Front wall, while the second half is a main flow stream reattaching the opposite Side wall and proceeding towards the Rear wall. This kind of a strong three-dimensional flow movement is paid by a large pressure drop increase, which is almost one order higher than as it would have been in a rectangular cross sectional flow channel.

60-deg. Proportional Ribs

A fundamentally almost identical flow structure as in the case of non-proportional ribs can be observed for the proportional ribs in Fig. 10. The flow between two consecutive ribs is divided into two flow fields, two counter rotating vortices, respectively. The only small difference is a smaller mass flow rata near the flow impinging rib side (represented by a smaller size of the flow velocity vectors), which is caused by 1) a wider space for the air flow between the rib and the opposite ribbed wall as a result of the proportional rib shape and 2) slightly weaker rotational momentum of the vortices.

In a closer look at the flow visualization and numerical simulation results in Fig. 11, one has to conclude that in contrast to

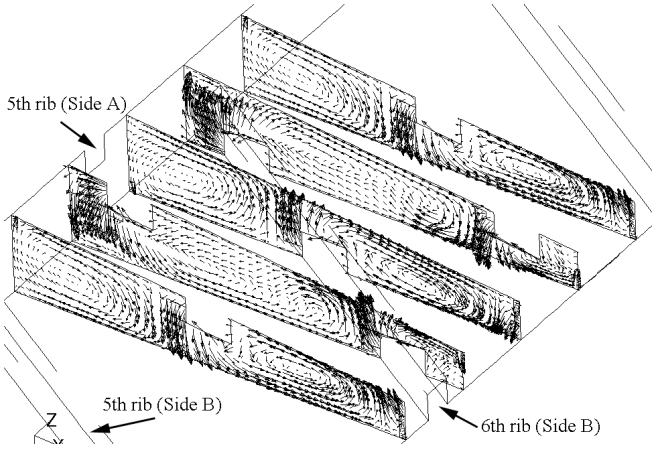

Fig. 9 Cross sectional velocity vector distribution between 5th, 6th and 7th ribs for 60-deg. non-proportional ribs, *Re*=15,000.

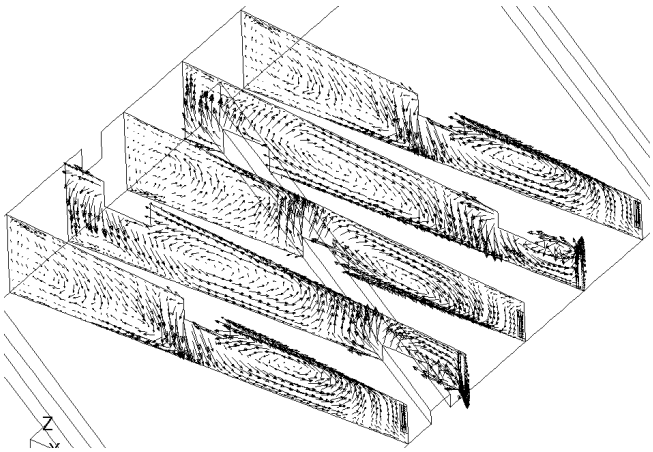

Fig. 10 Cross sectional velocity vector distribution between 5th, 6th and 7th ribs for 60-deg. proportional ribs, *Re*=15,000.

the non-proportional ribs, the proportional rib shape allows more air transfer near the Rear wall. This is indicated by: 1) a longer flow velocity vectors near the Front wall and 2) considerably smaller flow separations with flow reattachments taking place just behind the ribs instead of in front of the rib mounted on the opposite ribbed wall (see Figs. 11c1 and 11c2). However, the proportional rib height also deteriorates the strength of the secondary flow as it was indicated by the smaller velocity vector size of the vortices in Fig. 10 and as it can be confirmed by the smaller velocity vector inclination towards the Front wall in contrast to the non-proportional ribs. The rib proportional shape also considerably decreases the pressure drop in comparison to the 60-deg. non-proportional ribs due to larger area for the air flow.

45, 75-deg. Proportional and Non-Proportional Ribs

45, 75-deg. inclined rib arrangements induce generally the same flow structures as were presented for the 60-deg. proportional and non-proportional ribs. To the authors knowledge no significant differences could be observed for these rib arrangements except the velocity vector inclination and the strength of the secondary flow rotational momentum, which appreciably depends on the rib inclination. It was concluded that the strength of the secondary flow rotational momentum increases with the change of the rib inclination from 90→75→60→45-deg ribs, which coincides with the increasing velocity vector inclination towards the Rear wall.

CONCLUSIONS

The present study focuses on detailed examination of the flow behavior inside a high aspect ratio rib-roughened trapezoidal cooling channel (corresponding to a real cooling passage inside a turbine blade). The emphasis is placed on the experimental and numerical investigation of the rib-induced flow structures with two different types of ribs; non-proportional and proportional ribs, respectively, and four different rib inclinations, 90, 75, 60 and 45-deg. ribs. The following conclusions were drawn:

1) The 90-deg. proportional and non-proportional ribs induce a three-dimensional flow structure as a result of the trapezoidal channel shape in comparison to the two-dimensional flow phenomenon, flow separation and reattachment, respectively, observed for the square or rectangular cross sectional flow channels.

2) The 90-deg. proportional rib shape diminishes the proportion of the flow separations behind the ribs to the area taken by the main flow stream with the smallest flow separation occurring near the Front wall. In addition, it induces a considerably better air flow distribution and mass transfer near the Rear wall than in the case of the 90-deg. non-proportional ribs.

3) The inclined non-proportional ribs inside the trapezoidal flow channel induce a secondary flow, which conveys the air from the channel core regions towards the Rear wall. The secondary flow presses a larger volume of air towards the Rear wall and by doing so it enhances the air transfer at this region and diminishes the size of the local boundary layers.

4) The proportional ribs induce fundamentally almost identical flow structure as in the case of non-proportional ribs, but with a higher flow velocity, considerably smaller flow separations behind the ribs near the Rear wall and lower pressure drop. However, they also deteriorate the strength of the secondary flow rotational momentum as a result of the wider space for the air transfer between the rib and the opposite ribbed wall.

5) The strength of the secondary flow rotational momentum increases with the change of the rib inclination from 90→75→60→45-deg ribs which coincides with the augmentation of the secondary flow rotational momentum.

ACKNOWLEDGEMENTS

The authors would like to express their gratitude to Mr. Milan MATEJKA who was very helpful in carrying out the flow visualization experiments.

REFERENCES

Cheng, K. C., Shi, L., and Kurokawa, M., 1992, "Visualization of Flow Patterns in a 180-Degree Sharp Turn of a Square Duct", Proc. of 4th International Symposium on Transport Phenomena and Dynamics of Rotating Machinery, USA, Hawaii, vol. A, pp.124-132.

Dutta, S., Andrews, J.M. and Han, J.-C., 1996, "Prediction of Turbulant Flow and Heat Transfer in Rotating Square and Rectangular Smooth Channels", ASME Journal of Turbomachinery, No. 96-GT-234.

Dutta, S., Han, J.-C. and Zhang, Y.-M., 1995, "Influence of Rotation on Heat Transfer from a Two-Pass Channel with Periodically Placed Turbulence and Secondary Flow Promoters", International Journal of Rotating Machinery, vol. 1, pp. 129-144.

Ekkad, S. V. and Han, J.-C., 1997, "Detailed Heat Transfer Distribution in Two-Pass Square Channels with Rib Turbulators", International Journal of Heat and Mass Transfer, vol. 40, No. 11, pp. 2525-2537.

El-Husayni, H. A., Taslim, M. E. and Kercher, D. M., 1994, "Experimental Heat Transfer Investigation of Stationary and Orthogonally Rotating Asymmetric and Symmetric Heated Smooth and Turbulated Channels", Transactions of the ASME, vol. 116, pp. 124-132.

Cardone, G., Astarita, T. and Carlomagno, G. M., 1998, "Wall Heat Transfer in Static and Rotating 180-Degree Turn Channels by Quantitative Infrared Thermography", International Journal of Thermal Sciences, vol. 37, pp. 664-652.

60-deg. Proportional Ribs

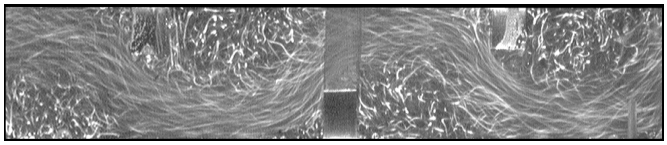

a1) Flow pattern taken at $x = 0.33w$ (near-Rear wall region).

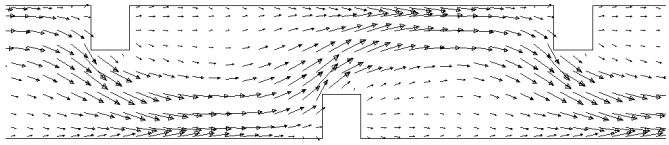

a2) Flow pattern taken at $x = 0.33w$ (near-Rear wall region).

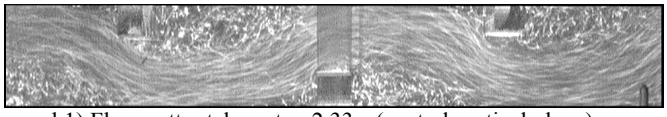

b1) Flow patter taken at x=2.33w (central vertical plane).

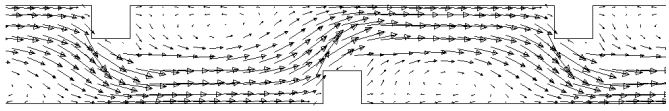

b2) Flow patter taken at x=2.33w (central vertical plane).

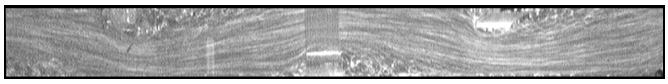

c1) Flow patter taken at x=4.66w (near-Front wall region).

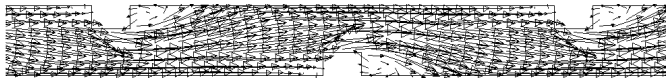

c2) Flow patter taken at x=4.66w (near-Front wall region).

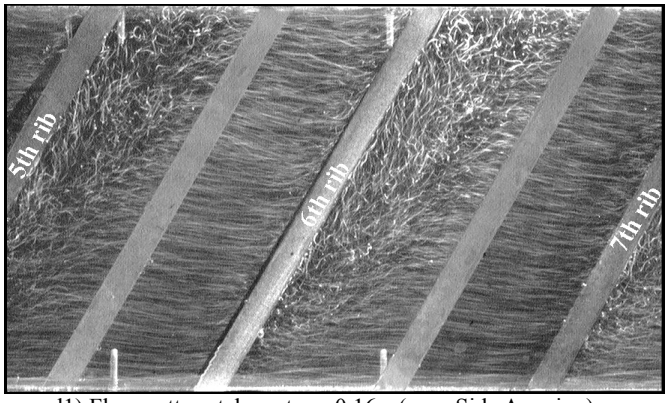

d1) Flow pattern taken at $y = 0.16w$ (near-Side A region).

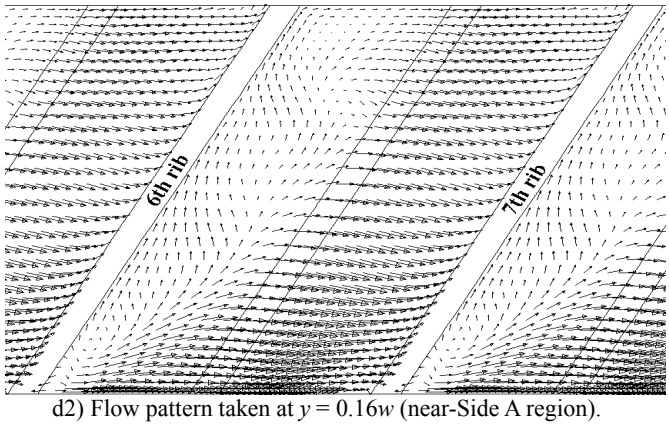

d2) Flow pattern taken at $y = 0.16w$ (near-Side A region).

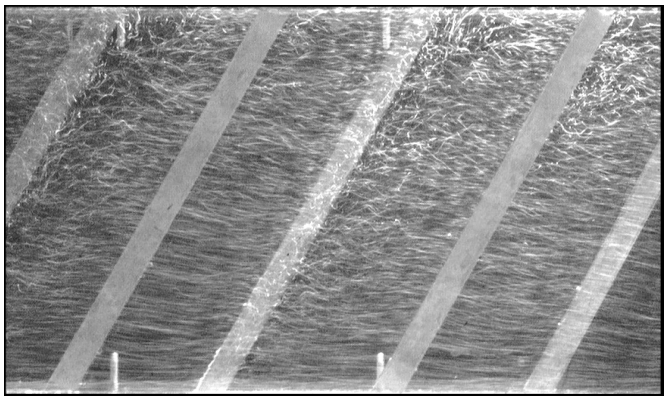

e1) Flow pattern taken at $y = 0$ (central horizontal plane).

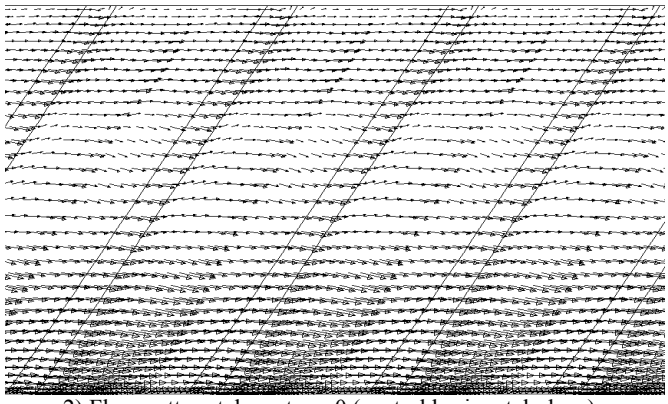

e2) Flow pattern taken at $y = 0$ (central horizontal plane).

Fig. 11 Velocity vector distribution between consecutive ribs for 60-deg. proportional ribs, *Re*=15,000.

Han, J.C., 1984, "Heat Transfer and Friction in Channels with Two Opposite Rib-Roughened Walls", ASME Journal of Heat Transfer, vol. 106, pp. 774-781.

Han, J.C., Park, J. S. and Lei, C. K., 1985, "Heat Transfer Enhancement in Channels with Rib Turbulence Promoters", ASME Journal of Engineering for Gas Turbines and Power, vol. 107, pp. 629-635.

Han, J.C., Zhang, Y.M. and Lee, C.P., 1991, "Augmented Heat Transfer in Square Channels with Parallel", Crossed, and V-Shaped Angled Ribs, ASME Journal of Heat Transfer, vol. 113, pp. 590-596.

Han, J.C. and Zhang, Y.M., 1992, "High Performance Heat Transfer Ducts with Parallel, Broken, and V-shaped ribs", International Journal of Heat and Mass Transfer, vol. 35, pp. 513-523.

Hirota, M., Fujita, H., Yokosawa, H. and Tanaka, Y., 1996, "Characteristics of Turbulent Flow in a Rectangular Duct with Rib-Roughened Long-Side Walls", Proc. of the 9th International Symposium on Transport Phenomena in Thermal-Fluids Engineering, Singapore, June 25-28.

Hu, Z. and Shen, J., 1996, "Secondary Flow and It's Contribution to Heat Transfer Enhancement in a Blade Cooling Passage with Discrete Ribs", Proc. of International Gas Turbine and Aeroengine Congress & Exhibition Birmingham, UK, June 10-13,.

Johnson, B.V., Wagner, J.H., Steuber, G.D. and Yeh, F.C., 1993, "Heat Transfer in Rotating Serpentine Passages with Selected Model Orientations for Smooth or Skewed Trip Walls", ASME Paper 93-GT-305.

Johnson , B.V., Wagner, J.H., Steuber, G.D. and Yeh, F.C., 1994, "Heat Transfer in Rotating Serpentine Passages with Trips Skewed to the Flow", ASME Journal of Turbomachinery, vol. 116, pp. 113-123.

Kawaike, K., Anzai, S., Takehara, I., Sato, M., Matsuzaki, H. and Kobayashi, Y., (1995) "Advanced Internal Cooling of Turbine Nozzles and Blades for 1500C-glass Gas Turbines", Proc. of International Gas Turbine Congress, Yokohama, Japan, October 22-27.

Kiml R., Mochizuki S. and Murata A., 1998, "Influence of 180 Degree Sharp Turn on the Heat Transfer and Flow Behavior in a Smooth Square Cross Sectional Serpentine Channel", 8th International symposium on Flow Visualization, CD Rom Proc. of 8th International Symposium on Flow Visualization, Sorrento, Italy, Paper's File No. 067, pp. 1-8.

Kiml, R., Mochizuki, S. and Murata, A., 2000, "Influence of the Gap Size between Side Walls and Ribs on the Heat Transfer in a Stationary and Rotating Straight Rib-Roughened Duct", International Journal of Rotating Machinery, vol. 6, No. 4, pp. 253-263.

Kiml, R., Mochizuki, S. and Murata, A., 2000, "Function of Ribs as Turbulators and Secondary Flow Inducers, 9th International symposium on Flow Visualization", CD Rom Proc. of 9th International symposium on Flow Visualization, Edinburgh, United Kingdom, Paper's File No. 164, pp. 1-10.

Kiml, R., Mochizuki, S. and Murata, A., 2001, "Heat Transfer Enhancement Mechanism in a Rectangular Passage with V- and Λ-Shaped Ribs", Journal of Flow Visualization and Image Processing, Vol. 8, pp. 51-68.

Kiml, R., Mochizuki, S. and Murata, A. 2001, "Effects of Gaps between Side-Walls and 60° Ribs on the Heat Transfer and Rib Induced Secondary Flow inside a Stationary and Rotating Cooling Channel", International Journal of Rotating Machinery, Vol. 7(6), pp. 425-433.

Kiml, R., Mochizuki, S. and Murata, A. 2001, "Effects of Rib Arrangements on Heat Transfer and Flow Behavior in a Rectangular Rib-Roughened Passage", Journal of Heat Transfer, Vol. 123, No. 4, pp. 675-681.

Kiml R., Mochizuki S. and Murata A., 2001, "Effects of Gaps between the Side-Walls and Ribs on the Rib Induced Secondary Flow", 6th Asian Symposium on Flow Visualization, CD-Rom Proceedings of 6th Asian Symposium on Flow Visualization, Bussan, South Korea, (18-31st May 2001), File No. 052, pp. 1-6.

Metzger, D. E., Plevich, C W. and Fan, C. S., 1984, "Pressure Loss Through Sharp 180 Degree Turn in Smooth Rectangular Channels", Trans. ASME Journal of Engineering for Gas Turbines and Power, vol. 106, pp. 677-681.

Mochizuki, S., Murata, A. and Fukunaga, M., 1997, "Effects of Rib Arrangement on Pressure Drop and Heat Transfer in a Rib-roughened Channel with a Sharp 180° Turn", ASME Journal of Turbomachinery, vol. 119, pp. 610-616,.

Murata, A., and Mochizuki, S., 2001, "Effect of Centrifugal Buoyancy on Turbulent Heat Transfer in an Orthogonally Rotating Square Duct with Transverse or Angled Rib Turbulators", International Journal of Heat Mass Transfer, vol. 44 (14), pp. 2739-2750.

Murata, A., Mochizuki, S. and Fukunaga, M., 1994, "Detailed Measurement of Local Heat Transfer in a Square-Cross-Section Duct with a Sharp 180-deg Turn, Proceedings of the 10th International Heat Transfer Conference", Brighton, United Kingdom, vol. 4, pp. 291-296.

Rau, G., Cakan, M., Moeller, D. and Arts, T., 1996, "The Effect of Periodic Ribs on the Local Aerodynamic and Heat Transfer Performance of a Straight Cooling Passage", Proc. of International Gas Turbine and Aeroengine Congress & Exhibition Birmingham, UK, June 10-13.

Taslim, M. E., Rahman, A. and Spring, S. D., 1991, "An Experimental Investigation of Heat Transfer Coefficients in a Spanwise Rotating Channel With Two Opposite Rib-Roughened Walls", ASME Journal of Turbomachinery, vol. 113, pp. 75-82.

Taslim, M. E., Li, T.. and Kercher, D. M., 1994, "Experimental Heat Transfer and Friction in Channels Roughened with Angled V shaped and discrete Ribs on Two Opposite Walls", ASME Paper 94-GT-163.

Taslim, M. E., Li, T. and Spring, S. D., 1995, "Measurements of Heat Transfer Coefficient and Friction Factor in Rib-Roughened Channels Simulating Leading-Edge Cavities of a Modern Turbine Blade", Journal Turbomachinery, vol. 119, pp. 601- 609.

Taslim, M. E., Li, T. and Spring, S. D., 1997, "Experimental Study of the Effects of Bleed Holes on Heat Transfer and Pressure Drop on Trapezoidal Passages With Tapered Turbulators", Journal Turbomachinery, vol. 117, pp. 281- 289.

Wagner, J. H., Johnson, B. V., Graziani, R. A. and Yeh, F. C., 1992, "Heat Transfer in Rotating Serpentine Passages With Trips Normal to the Flow", ASME Journal of Turbomachinery, vol. 114, pp. 847-457.

Zhang, Y. M., Gu, W. Z. and Han, J. C., 1994, "Heat Transfer and Friction in Rectangular Channels Ribbed and Ribbed-Grooved Walls", ASME Journal of Heat Transfer, vol. 116, pp. 58-65.